

DFT STUDY ON THE INTERACTIONS OF LOW ENERGY ELECTRONS WITH PYRIDINE, PYRAZINE, AND THEIR HALO DERIVATIVES

Natalia Tańska¹

¹*Institute of Physics and Applied Computer Science, Faculty of Applied Physics and Mathematics, Gdańsk University of Technology, ul. Gabriela Narutowicza 11/12, 80-233 Gdańsk
E-mail: natalia.tanska@pg.edu.pl*

Vertical electron affinities to pyridine, pyrazine and their halo-monosubstituted derivatives were calculated with density functional theory using B3LYP hybrid functional and various basis sets. Relaxed potential energy curves along C-X (X=H, Cl, Br) bond and enthalpies of dissociative attachment of thermal electron to the investigated molecules were also determined to roughly estimate the energetics of the process. The results are in acceptable agreement with the available data.

1. Introduction

Dissociative electron attachment (DEA), shown schematically in the Figure 1, plays a significant role in both science and industry [1]. This chemical reaction control tool is used in the FEBID (Focused Electron Beam Induced Deposition) method [2] or radiotherapy [3]. DEA manifests itself also in many astrophysics and astrochemical processes, for example in auroras of Earth and other planets and in formation of complex molecules in atmospheres, comets and interstellar medium [4]. In many of the above fields, organic or biological molecules are of particular importance.

Potential energy curves (PECs) are very helpful in understanding the dissociative electron attachment, as well as other chemical reactions. To calculate PECs that are useful in electron scattering processes, one should use a sophisticated method such as R-matrix theory [5] or multichannel Schwinger method [6]. Unluckily, each has its flaws, including the need of large computing resources or even fine-tuning to the experimental data to achieve meaningful results. On the other hand, simple and relatively efficient methods of quantum chemistry, such as the second order Møller-Plesset perturbation theory (MP2) or the density functional theory (DFT), can lead to erroneous results when dealing with temporary negative ions (TNIs). This is caused by the fact that the structure is not stable and the calculations could locate the extra electron on a very diffuse orbital. Quite acceptable results can be achieved by using a compromise between the size of the base orbitals and the accuracy of calculations, which has been shown in [7,8]. Pyridine and pyrazine rings are present for example in B vitamins, pharmaceuticals and agrochemicals. As one of the simplest biological molecules, pyridine is considered in astrochemical experiments [9] and nucleic acids based on pyrazine are candidates for the prebiotic RNA precursor [10]. In this work we apply the DFT method with B3LYP functional to obtain the vertical electron affinities (VEAs) and potential energy curves for pyridine, pyrazine and those molecules monosubstituted by chlorine or bromine atom.

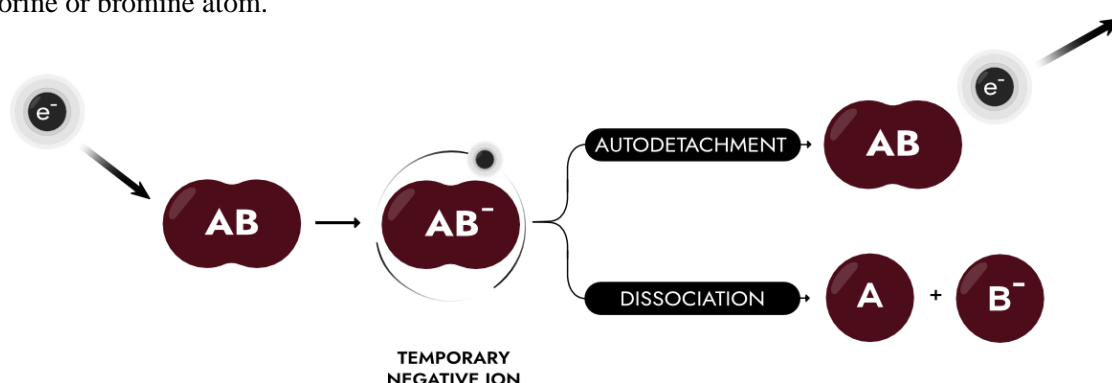


Fig. 1. Schematic representation of the dissociative electron attachment.

2. Details of calculations

All calculations were performed with Gaussian 16 suite. The vertical electron affinities for 2-,3- or 4-substituted pyridines and 2-substituted pyrazines were obtained with basis sets listed in the Table 1 with the B3LYP functional according to the formula:

$$VEA = E(\text{neutral}) - E(\text{anion}) \quad (1)$$

where both of the species are in the optimized neutral geometry. Singly occupied molecular orbitals (SOMOs) were then carefully inspected for the correct symmetry and size, that is, whether they are the resonant π^* orbitals of b_1 or b_1 -like symmetry. Relaxed potential energy curves along the C_n-X bond (for the numbering of atoms see Figure 2) were calculated with Opt = ModRedundant keyword at the B3LYP/6-31+G(d) level. Separate scans were performed for the neutral molecule, anion lowest π^* state, σ^* dissociative state and π^*/σ^* mixed (without any symmetry constraints). The enthalpies of the following reactions were also determined:



where $X=Cl, Br$ and e_0^- is the thermal (near-zero eV) electron.

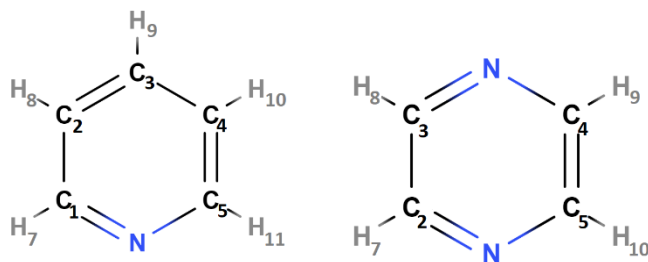


Fig. 2. The numbering of atoms in pyridine and pyrazine used in this work.

3. Results and conclusions

Calculated vertical electron affinities are shown in the Table 1. In the Figure 3 the discrepancies between obtained values and experimental data are depicted. The only available data that concern halo derivatives of investigated compounds are for 2-,3-, and 4-chloropyridine and for 4-bromopyridine. For the 6-31+G(d) and aug-cc-pVTZ the trend is correct and the agreement is acceptable. The 6-311++G(d,p) basis was problematic during the calculations because of the deformed orbitals, and so the results are less predictable.

Tab. 1. Calculated vertical electron affinities (eV). Two values are given if the lowest in energy SOMO is diffuse and has different symmetry than $\pi^*(b_1)$.

	6-31G(d)	6-311G(d,p)	6-31+G(d)	6-311++G(d)	aug-cc-pVTZ
Py	-1.68	-1.31	-0.93	-0.31 or -0.65	-0.35 or -0.85
2-ClPy	-1.16	-0.76	-0.55	-0.49	-0.49
2-BrPy	-1.11	-0.77	-0.5	-0.43	-0.42
3-ClPy	-1.16	-0.76	-0.53	-0.47	-0.46
3-BrPy	-1.11	-0.77	-0.48	-0.41	-0.4
4-ClPy	-1.18	-0.82	-0.52	-0.48	-0.44
4-BrPy	-1.11	-0.76	-0.41	-0.37	-0.36
Pz	-0.97	-0.67	-0.27	-0.22	-0.22
2-ClPz	-0.47	-0.17	0.10	0.15	0.14
2-BrPz	-0.41	-0.13	0.15	0.22	0.20

In the case of pyridine in the two biggest basis, the order of the orbitals is changed and the lowest energy SOMO has incorrect symmetry, values of VEAs to both orbitals are given in the table. It can be seen that the VEAs tend to converge to the fixed values with increasing basis set and that the 6-31+G(d) is sufficient, not problematic and compact at the same time.

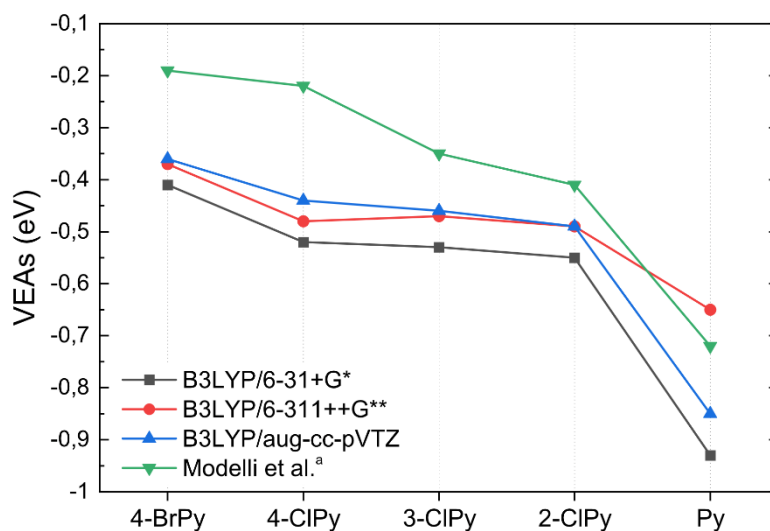


Fig. 3. Vertical electron affinities obtained in different basis sets comparing to the experimental data.
^aVEAs from [11] and [12].

Potential energy curves for pyridine, pyrazine, halopyrazines and 4-substituted pyridines, are shown in the Figures 4-6. Mulliken population analysis revealed, that if the bond C-X is stretched (X=H, Cl, Br), the extra electron rather resides on the ring, in case of pyridine and pyrazine, or on the halogen atom in substituted compounds, following the reactions from Eq. (2) and Eq. (3), respectively. Enthalpies of these reactions are listed in the Table 2 along with the equilibrium lengths of C-X bonds in neutral molecules. All the anion curves without symmetry constraints are qualitatively the same. They start with planar geometry and π^* state. Close to the intersection of the π^* and σ^* states, the states mix by the deviation of the C_n-X bond from the plane of the ring to about 40° , to finally form the σ^* state of planar geometry and the molecule dissociates. The curves of pyridine and pyrazine are also quantitatively similar, except that the curve of pyrazine anion lies very close to the neutral one. This is reflected in the results of other research groups showing the adiabatic affinity of pyrazine is close to zero (e.g. [13]). Formation of the $[\text{Py-H}]^-$ anion was observed at 2.5 eV by Ryszka and coworkers [14], so quite below the reaction threshold. Both dissociation to the σ^* state and the π^* state are highly energy unfavourable. According to calculations, anions of halopyrazines are stable with respect to the neutral molecule and dissociation products of the reaction in Eq. (2). Unfortunately, there is no experimental or theoretical data with which to compare that result. Halopyridines have negative vertical electron affinities and do not have a clear minimum in π^* state. The minimum of σ^* state is visible, but rather shallow. Formation of Cl^- and Br^- from 4-chloropyridine and 4-bromopyridine was observed by Modelli et al. [12] at 0.26 eV and 0.1 eV, respectively. This is in a good agreement with VEAs obtained by this group, indicating that the curve may be (almost) repulsive. Enthalpies of reaction in Eq. (3) are relatively small or negative for 2-substituted halopyridines and halopyrazines.

Tab. 2. Calculated parameters of the potential energy curves. AE is the activation energy (kcal/mol), $r(C_n-X)$ is the equilibrium distance in the neutral molecule (Å) and ΔH (kcal/mol) stands for the enthalpy of reactions in Eq. (2) and Eq. (3).

	AE	$r(C_n-X)$	ΔH	
	6-31+G(d)	6-31+G(d)	6-31+G(d)	aug-cc-pVTZ
2-HPy	-	1.0887	86.4	86.4
3-HPy	-	1.0865	78.2	78.8
4-HPy	-	1.0872	76.1	76.7
2-ClPy	1.38	1.7622	-0.104	1.40
2-BrPy	0.00	1.9111	0.174	-7.69
3-ClPy	1.18	1.7536	3.20	4.97
3-BrPy	0.00	1.8986	4.17	-3.61
4-ClPy	0.00	1.7524	2.62	4.39
4-BrPy	0.00	1.8975	3.42	-4.41
Pz	-	1.0881	77.5	78.0
2-ClPz	5.78	1.7533	-0.763	0.763
2-BrPz	3.79	1.9019	-0.570	-8.21

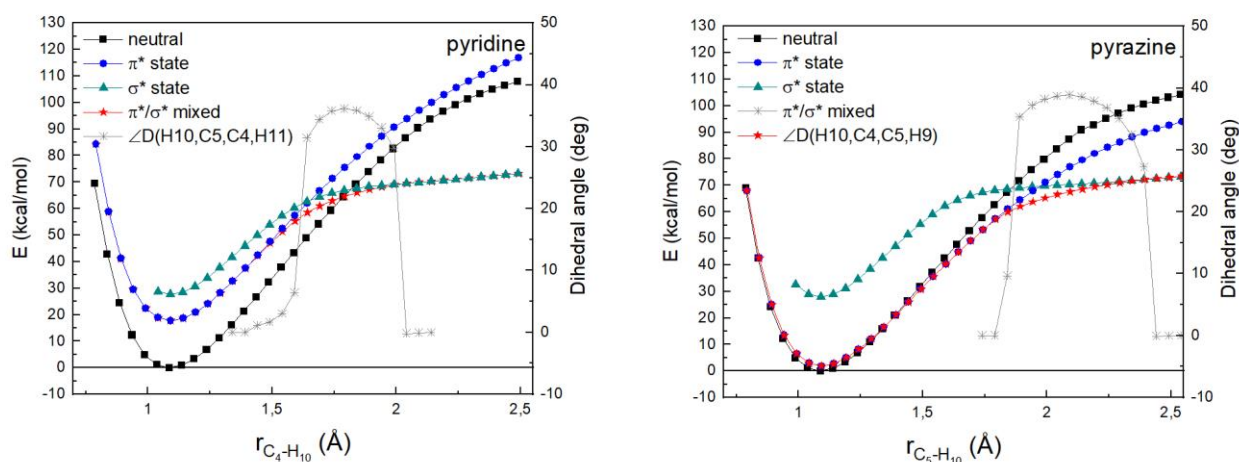


Fig. 5. Potential energy curves of pyridine and pyrazine. Numbering of atoms is in the Figure (2).

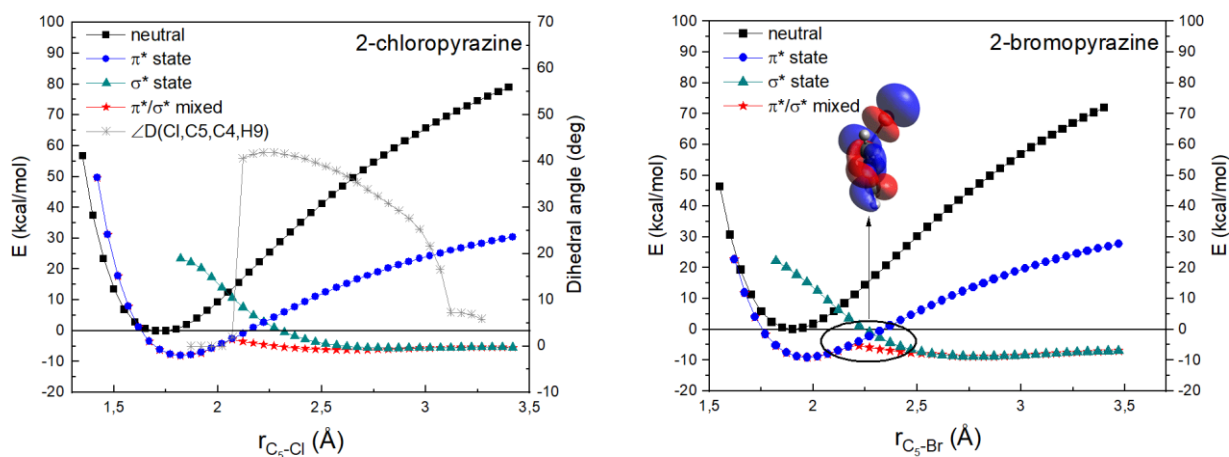


Fig. 4. Potential energy curves of halopyrazines. On the right the area of the bond bending is circled and the mixed π^*/σ^* orbital is shown.

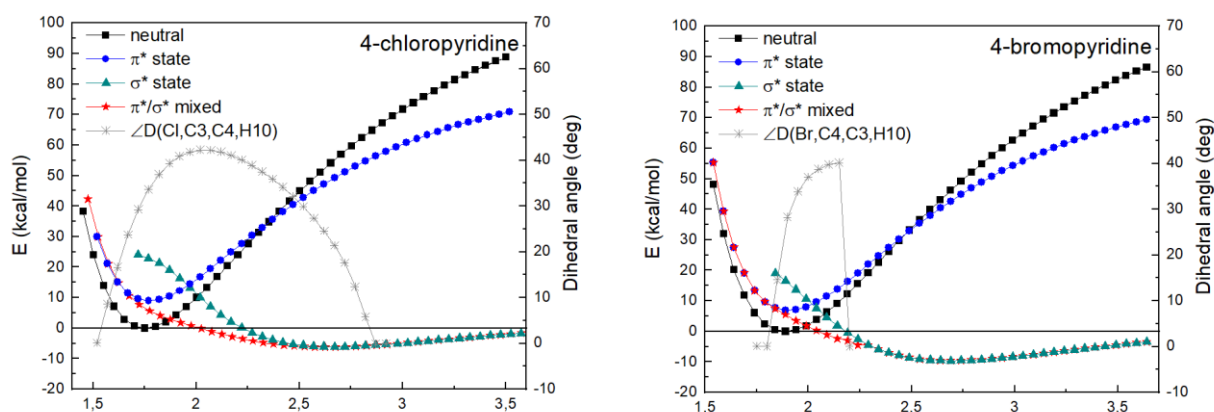


Fig. 6. Potential energy curves of halopyridines.

4. Summary

Determining the vertical electron affinity using the B3LYP functional with the basis set that includes diffuse functions can be an alternative to the more sophisticated ones, but the SOMO orbital should be carefully verified. According to calculations, pyrazine has a near-zero adiabatic electron affinity, halopyrazines form stable anions, whereas negative ions of pyridines are temporary. Dissociation of the investigated molecules goes through the symmetry breaking by bending of the dissociating bond, and therefore converting from the π^* to σ^* state. The curves of halopyridines may be almost repulsive. Dissociative attachment of the thermal electron for 2-substituted molecules is slightly endothermic or exothermic, while for pyridine and pyrazine molecules highly endothermic.

5. Acknowledgments

Calculations were carried out at the Academic Computer Centre in Gdańsk (TASK).

6. References

- [1] Fabrikant I I, Eden S, Mason N J and Fedor J 2017, Recent Progress in Dissociative Electron Attachment: From Diatomics to Biomolecules, in: *Advances In Atomic, Molecular, and Optical Physics*, Vol. 66, edited by Arimondo E, Lin C C and Yelin S F, Academic Press, pp. 545-657
- [2] Huth M, Porrati F and Dobrovolskiy O 2018 *Microelectron. Eng.* **185-186** 9
- [3] Chen H-Y, Chen H-F, Kao C-L, Yang P-Y, Hsua S C N 2014 *Phys. Chem. Chem. Phys.* **16** 19290-19297
- [4] Joshipura K, Mason N 2019, Applications of Electron Scattering, in: *Atomic-Molecular Ionization by Electron scattering: Theory and Applications*. Cambridge University Press, Cambridge, pp. 177-218
- [5] Burke P G 2011, *R-Matrix Theory of Atomic Collisions*. Springer, Berlin, Heidelberg
- [6] Winstead C and Mckoy V 1996 *Adv. Atom. Mol. Phys.* **36** 183
- [7] Szarka A Z, Curtiss L A and Miller J R 1999 *Chem. Phys.* **246** 147
- [8] Mishra P M 2015, *Comput. Theor. Chem.* **1068** 165
- [9] McMurtry B M, Turner A M, Saito S E and Kaiser R I 2016 *Chem. Phys.* **472** 173
- [10] Weber A L 2008 *Org. Life Evol. Biosph.* **38** 279
- [11] Modelli A and Burrow P D 1983 *J. Electron Spectros. Relat. Phenomena* **32** 263
- [12] Modelli A, Foffani A, Scagnolari F and Jones D. 1989 *Chem. Phys. Lett* **163** 269
- [13] Mašin Z and Gorfinkiel J D 2011 *J. Chem. Phys.* **135** 144308
- [14] Ryszka M, Alizadeh E, Li Z and Ptasińska S 2017 *J. Electron, Spectros. Relat. Phenomena* **147** 094303